



1  
2  
3  
4  
5  
6  
7

## Open access resources on motion artifact in adult dentomaxillofacial CBCT: illustrated pictorial review of medical literature

---

Authors:  
Olszewski R DDS, MD, PhD, DrSc<sup>1,\*2</sup>

8

### Affiliations:

9  
10  
11  
12  
13  
14  
15  
16

<sup>1</sup> Department of Oral and maxillofacial surgery, Cliniques universitaires saint Luc, UCLouvain, Brussels, Belgium

<sup>2</sup> Oral and maxillofacial surgery research Lab, NMSK, IREC, SSS, UCLouvain, Brussels, Belgium

\*Corresponding author: Pr R. Olszewski, Department of Oral and maxillofacial surgery, Cliniques universitaires saint Luc, UCLouvain, Brussels, Belgium, phone+3227645718; fax: +3227645876; ORCID iD: [orcid.org/0000-0002-2211-7731](https://orcid.org/0000-0002-2211-7731)

17  
18  
19

Disclaimer: the views expressed in the submitted article are our own and not an official position of the institution or funder.

20

## Abstract

21

**Objective:** to know how much open access/open knowledge reference figures were available on motion artifacts in CBCT dentomaxillofacial imaging, and to describe and to categorize clinical variation of motion artifacts related to diverse types of head motion retrospectively observed during CBCT scanning time.

22

23

24

25

26

27

28

29

30

31

32

33

34

35

**Material and methods:** a search equation was performed on Pubmed database. We found 56 articles. The 45 articles were out of scope, and 7 articles were excluded after applying exclusion and inclusion criteria. Only 4 articles were finally freely accessible and selected for this review. Moreover, we retrospectively used our department CBCT database to search examinations with motion artifacts. We also checked retrospectively for radiological protocols as the type of motion artifact was described when occurred during the CBCT scanning time by the main observer. We had obtained the approval from the Ethical committee for this study.

36

37

38

39

40

41

42

**Results:** The accessibility of free figures on motion artifact in dentomaxillofacial CBCT is limited to 13 figures not annotated, and to one annotated figure presenting a double contour around cortex of bony orbits. We proposed to categorize the motion artifacts into three levels: low, intermediary, and major. Each level was related to: 1) progressive image quality degradation, 2) distortion of anatomy, and 3) potential possibility of performing clinical diagnosis. All 45 figures were annotated.

43

44

45

46

47

48

49

50

51

52

53

**Conclusions:** There exists a scarce open access literature on motion artifacts in CBCT. In our pictorial review we found that low level motion artifacts were more related to head rotation in axial plane (rolling). Rolling and lateral translation were responsible of intermediary level motion artifacts. Major level motion artifacts were created by complex motion with multiple rotation axes, multiple translation directions, and by anteroposterior translation. The main limitation of this study is related to retrospectively report empirical observation of patient motion during CBCT scanning and to compare these observations with motion artifacts found on clinical images. More robust methodology should be further developed using a virtual simulation of various types of head movements and associated parameters to consolidate the open knowledge on motion artifacts in dentomaxillofacial CBCT.

54

55

56

**Keywords:** CBCT, motion artifacts, patient movement, image quality, open access medical images

57

58

## Introduction

59

60

61

62

63

64

65

66

67

68

69

70

71

72

73

74

75

76

77

78

79

80

81

82

83

Motion artifacts present the 4<sup>th</sup> dimension in cone beam computed tomography (CBCT). Their presence may degrade image quality and image interpretation, and may require to retake CBCT thus increasing the absorbed dose to the patient. The prevalence of movement artifact in CBCT examinations depends on studies, and varies between 20% (patient monitoring) and 41% (motion artifact recognition) of cases [1]. Motion artifact is known to be related to physiological event such as breath, heart beating, unintentional tremor, and swallowing during CBCT scanning time [2]. Motion artifacts are more frequent in sitting and standing position CBCT [3, 4]. They can be also related to mechanical factors (cotton roll, head stabilization) [4, 5]. They are also more present in the beginning of the scanning time by surprising the patient by the noise and vibration [4, 6]. Motion artifacts are more related to specific group of age with patients less than 16 years and more than 65 years [4, 7]. Motion artifacts are related to longer scanning time [4, 8] to bigger size of field of view [4, 5], and to higher spatial resolution [9].

Thus open access and open knowledge on motion artifacts should be granted in medical literature to provide with annotated reference figures to recognize these important artifacts by the community of practitioners.

The purpose of our study was twofold. First we wanted to know how much open access/open knowledge and reference images were available for private practitioners on motion artifacts in CBCT dentomaxillofacial imaging. According to previous studies on availability of open knowledge on CBCT dentomaxillofacial imaging [10, 11], our null hypothesis was that there was scarce information available for free in the medical literature for dentists on this issue. We also wanted to describe and categorize great clinical variation of motion artifacts related to diverse types of head motion observed during CBCT scanning time.

84

## Materials and methods

85

86

87

88

89

90

91

92

93

94

95

We used PubMed database (free database) with the private access to be in the same situation as dentists from private practice. The search equation was set as follow: ("motion"[MeSH Terms] OR "motion"[All Fields]) AND ("artifacts"[MeSH Terms] OR "artifacts"[All Fields] OR "artifact"[All Fields]) AND CBCT[All Fields] AND "loattrfree full text"[sb]. The search was performed on 12.02.2020. One observer performed the search.

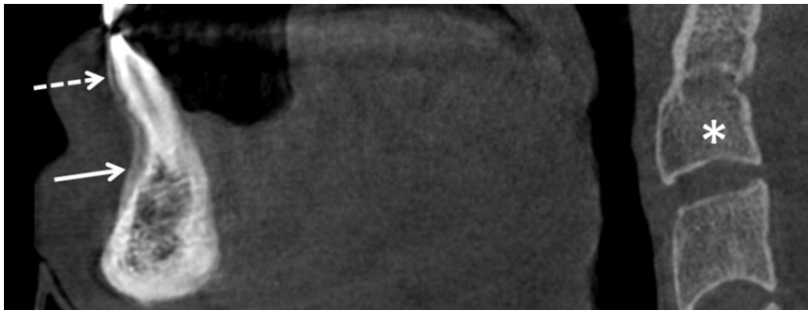
The Inclusion criteria were: free full text articles related to motion artifacts in CBCT in humans. The exclusion criteria were: closed access articles, articles not related to motion artifacts in CBCT, experimental articles, and articles related to animals. Two languages were selected: French and English. We found 56 articles. The 45 articles were out of scope, and 7 articles were excluded after applying exclusion and

96 inclusion criteria. Only 4 articles were finally freely accessible and selected for this  
97 review [12-15].  
98 Moreover, we retrospectively used our department CBCT database to search  
99 examinations with artifacted images to provide a broader spectrum of motion  
100 artifacts variation. We checked retrospectively for 2200 radiological protocols (from  
101 2018 to 2020) as the type of motion artifact was described by the main  
102 observer when occurred during the CBCT scanning time. We obtained the approval  
103 from our Ethical committee for this study (B403/2019/03DEC/542). We propose to  
104 separate the importance of motion artifacts into three levels: low, intermediary, and  
105 major. Each level was related to: 1) progressive image quality degradation, 2)  
106 progressive distortion of anatomy, and 3) potential possibility of performing clinical  
107 diagnosis. All figures were annotated.

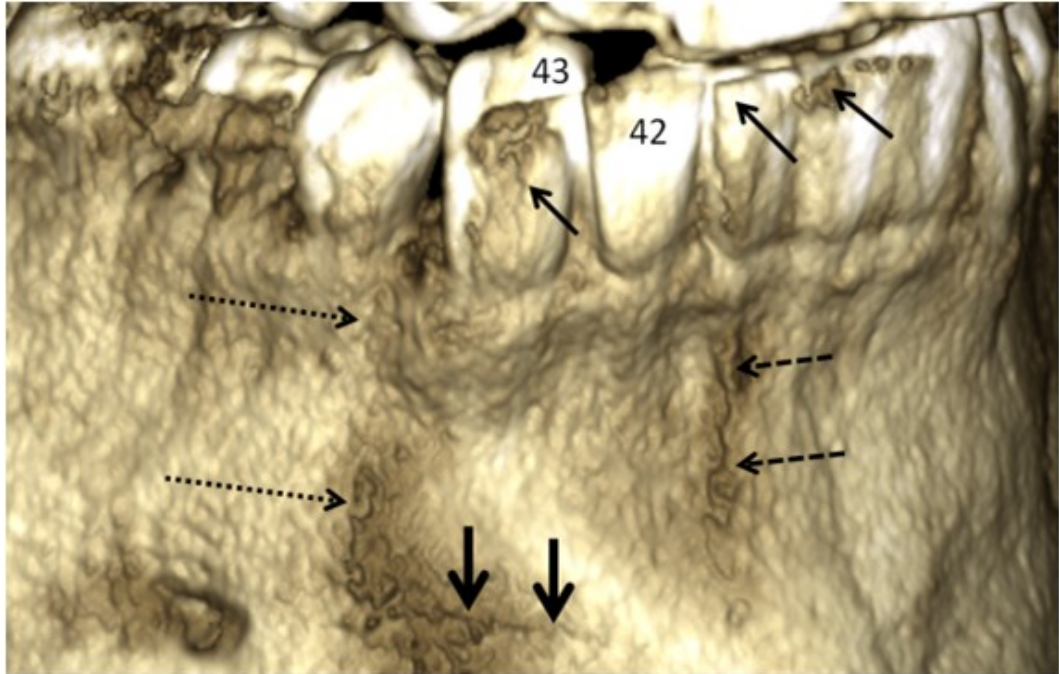
## 108 Results

109 The accessibility of free figures on motion artifact in dentomaxillofacial CBCT is  
110 limited to 13 not annotated figures, and to one annotated figure presenting a double  
111 contour around cortex of bony orbits [article 24]. We found 278 CBCT  
112 examinations with motion artifacts described in the radiological protocol out of 2200  
113 CBCT examinations from our department database (12.6%).

### 114 Motion artifacts of low level



115 **Fig. 1.** Patient 1. Sagittal view of the mandible and of the cervical spine.  
116 Arrow: duplication of the contour on vestibular side of the mandible. Dashed  
117 arrow: duplication of the contour of the incisor on vestibular side. No double  
118 contour around the chin. \* No motion of the cervical spine.  
119  
120



121  
122  
123  
124  
125  
126  
127  
128

**Fig. 2.** Patient 1. Head rotation from left to right. Three-dimensional (3D) reconstruction of the anterior mandible. Thick arrows: inferior limit of duplicated contour. Dashed arrows: vertical limit of the double contour at the level of tooth n°41. Dotted arrows: vertical limit of the double contour posterior to tooth n°43. Thin arrows: 3D reconstruction of double contour superimposed on the vestibular side of teeth n°31, 41, and 43.

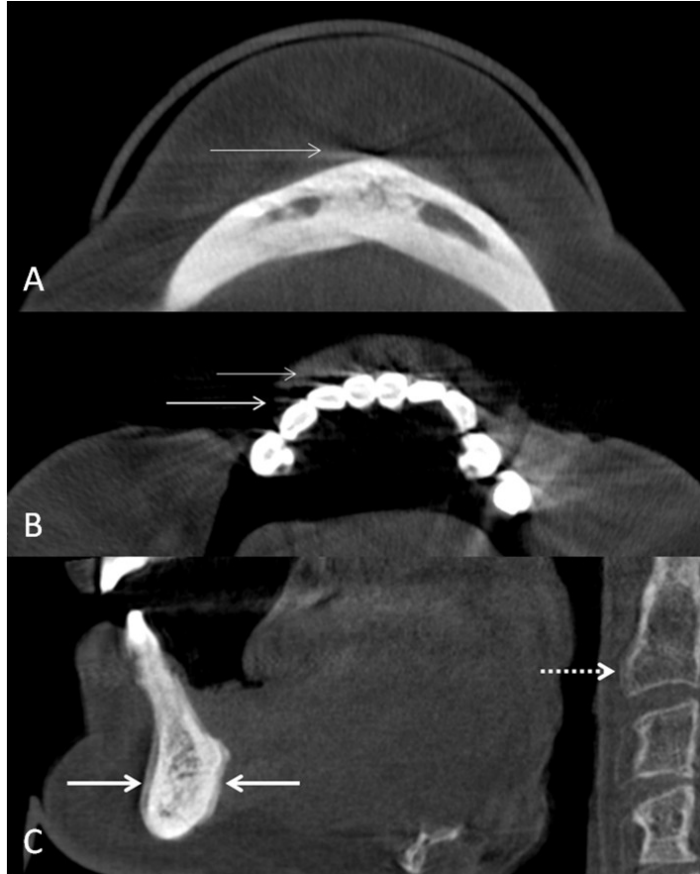
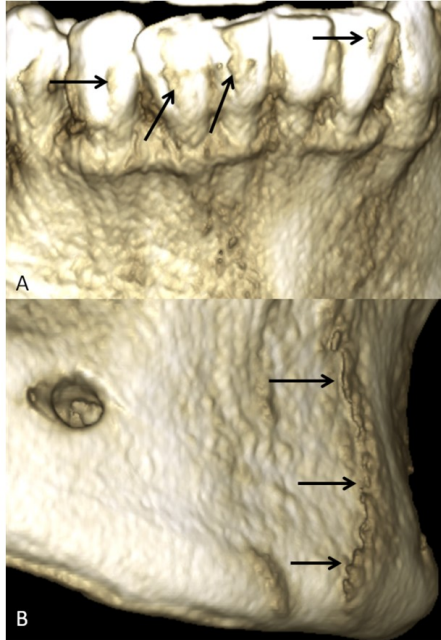


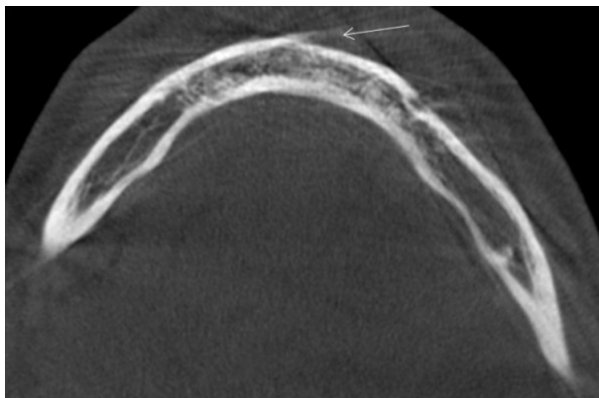
**Fig. 3.** Patient 2. Head rotation from left to right. A. Axial view of the mandible at the chin level. Arrow: thin streak tangent to bone area, and oriented to the right side. B. Axial view of the mandible at teeth level. Arrow: thin streak tangent to teeth crowns, and oriented to the right side. C. Sagittal view of the mandible, and of the cervical spine. Arrows: double contour around the mandibular chin area. Dotted arrow: absence of double contour around cervical vertebrae (no spine motion).

129  
130  
131  
132  
133  
134  
135  
136  
137  
138  
139  
140  
141  
142  
143



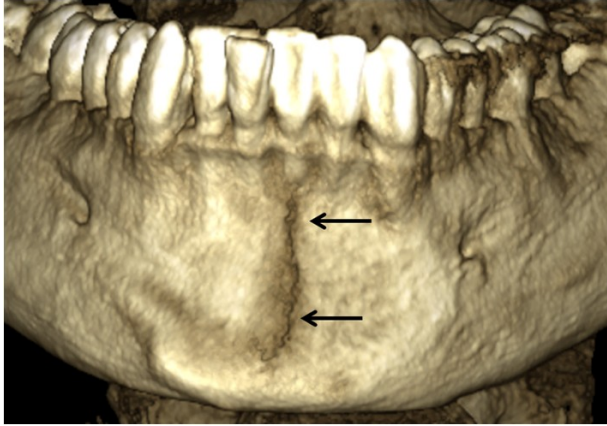
144  
145  
146  
147  
148  
149  
150  
151

**Fig. 4.** Patient 2. Head rotation from left to right. 3D reconstruction of the mandible. A. Frontal view of mandibular teeth. Black arrows: additional streaks on vestibular crown side of lower incisors and canine, and oriented to the right side. B. Right lateral view of the mandible chin area. Black arrows: 3D reconstruction of the motion streaks tangent to the vestibular cortical bone, and oriented to the right side.



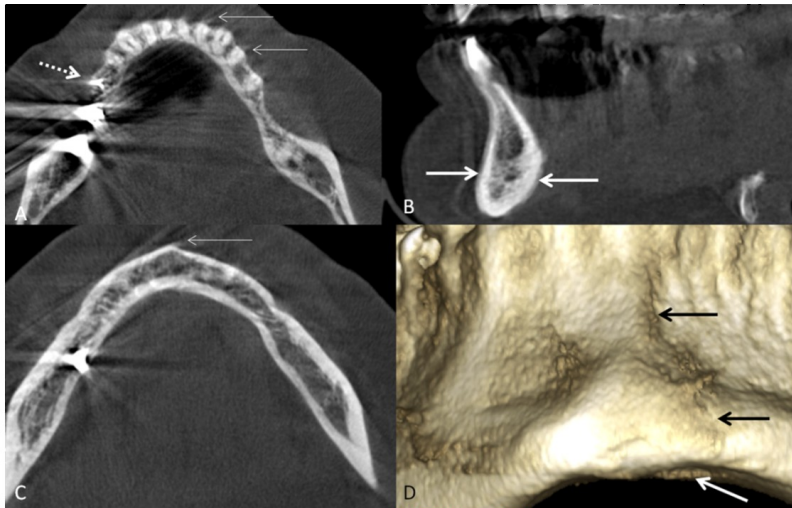
152  
153  
154  
155  
156

**Fig. 5.** Patient 3. Head rotation from right to left. Axial view of the mandible at the level of the chin. Thin arrow: thin streak tangent to the chin area, and oriented to the left.



157  
158  
159  
160  
161

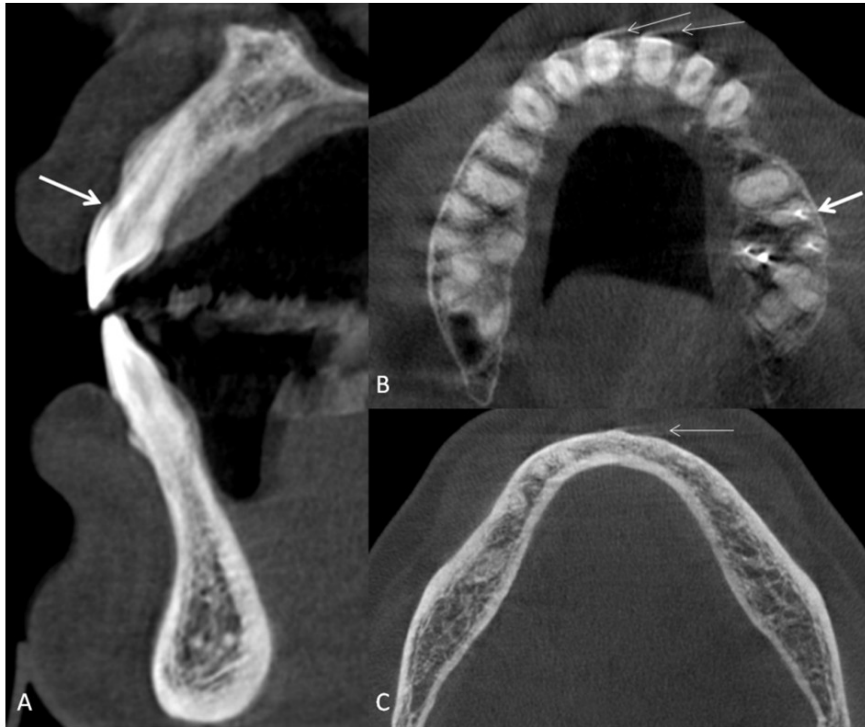
**Fig. 6.** Patient 3. Head rotation from right to left. 3D reconstruction of the mandible, anterior view. Black arrows: a line of fine streaks tangent to the vestibular cortical bone, and oriented to the left.



162  
163  
164  
165  
166  
167  
168  
169  
170  
171  
172

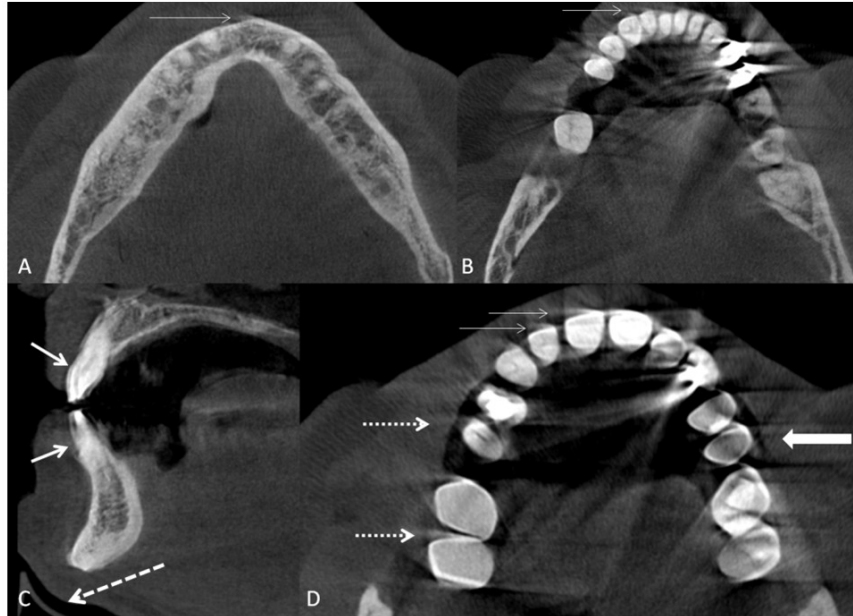
**Fig. 7.** Patient 4. Head rotation from right to left, and translation from right to left. A. Axial view of the mandible at the level of dental roots. Arrows: streak tangent to the vestibular side of tooth crown. Dotted arrow: Y-shaped artifact of the endodontic canal filling, oriented to the left. B. Sagittal view of the mandible. Arrows: minimal double contour around the chin area and around front teeth. C. Axial view of the mandible at the chin level. Thin arrow: thin streak tangent to the chin area, and oriented to the left. D. 3D reconstruction of the chin. Black arrows: line corresponding to the streaks tangent to the chin. White arrow: double contour of the cortical bone on the left side (translation right to left effect).

173

**Motion artifacts of intermediary level**

174  
 175  
 176  
 177  
 178  
 179  
 180  
 181  
 182  
 183

**Fig. 8.** Patient 5. Head rotation from right to left. A. Frontal view of the maxilla and of the mandible. Arrow: minimal double contour around the upper incisor. B. Axial view of the maxilla. Thin arrows: thin streak tangent to teeth crowns and oriented to the left side. Thicker arrow: Y-shaped artifact of the endodontic root filling. Y shape is oriented to the left. Loss of pulp chamber image for premolars and molars on right and left side. C. Axial view of the mandible at the chin level. Arrow: minimal thin streak tangent to bone area and oriented to the left side.

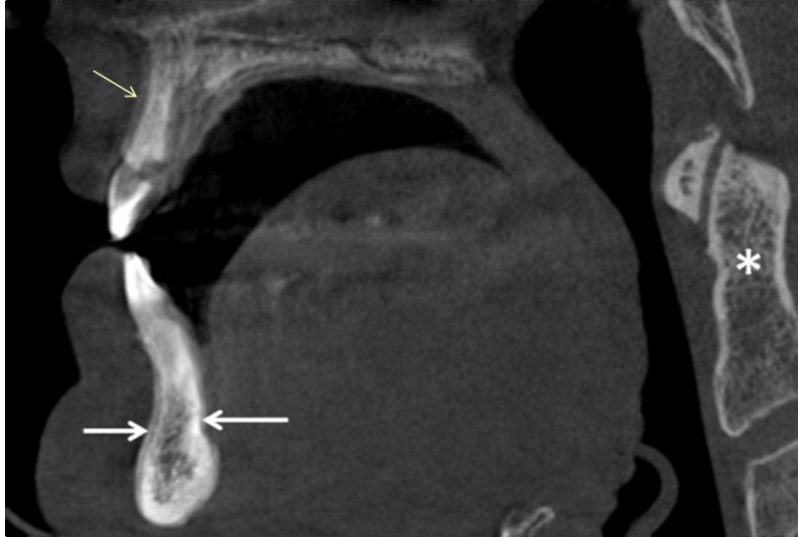


184  
 185 **Fig. 9.** Patient 6. Head rotation and translation from left to right. A. Axial view  
 186 of the mandible at the level of dental roots. Arrow: minimal streak tangent to  
 187 the chin area, and oriented to the right. B. Axial view of mandible at the level  
 188 of teeth crowns. Arrow: minimal streak tangent to vestibular side of anterior  
 189 teeth, and oriented to the right. C. Sagittal view of the maxilla and of the  
 190 mandible. Arrows: minimal double contours around front teeth. Dotted arrow:  
 191 soft tissue chin is not in contact with the plastic chin support. D. Axial view  
 192 of the maxilla at the level of teeth crowns. Thin arrows: minimal streaks tangent  
 193 to vestibular side of anterior teeth crowns. Thick arrow: large stripe  
 194 corresponding to the translation movement from left to right. Dotted arrows:  
 195 streak tangent to the lateral side of the tooth crown at the side of the end of  
 196 translation movement.  
 197  
 198  
 199  
 200  
 201  
 202  
 203  
 204  
 205  
 206  
 207  
 208  
 209



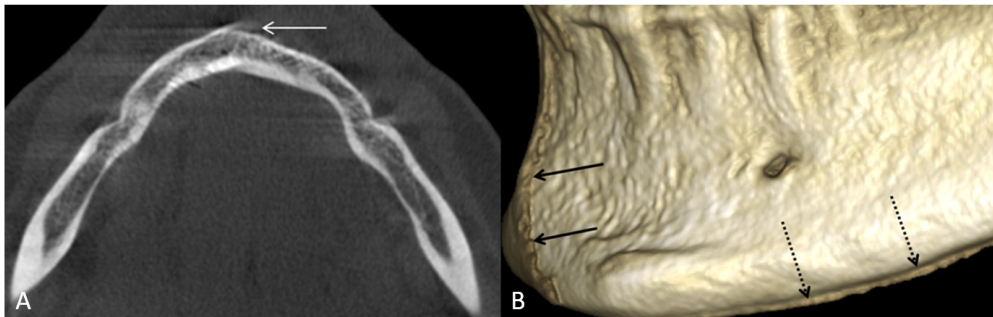
210  
211  
212  
213  
214  
215  
216  
217  
218  
219  
220  
221  
222  
223  
224  
225  
226  
227  
228  
229  
230  
231  
232  
233  
234

**Fig. 10.** Patient 6. Head rotation and translation from left to right. 3D reconstruction of maxillary and mandibular front teeth. A. Anterior view. Arrows: 3D reconstructed streaks on the vestibular side of teeth n°11, 12, and 13, and oriented to the right. B. Anterior view. White arrows: 3D reconstructed streaks on the vestibular side of teeth n°11, and 12, and oriented to the right. C. Anterior view on the mandibular chin area. Arrow: partial vertical line corresponding to thin streaks tangent to the bone. D. Anterior view of the mandible teeth. Black arrows: 3D reconstructed streaks on the vestibular side of teeth n°31, 41, 42, and 43, and oriented to the right.



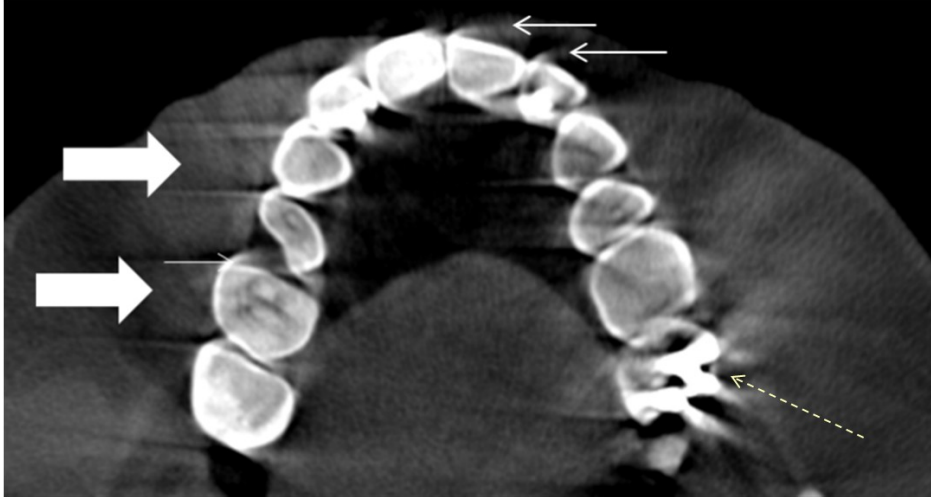
235  
236  
237  
238  
239  
240  
241

**Fig. 11.** Patient 7. Rotation from right to left, and translation from right to left. Sagittal view of the mandible, the maxilla and of the cervical spine. Thin arrow: double contour on the vestibular side of the maxilla. Thicker arrows: double contour on the vestibular and lingual side of the mandible. \* No motion at the level of the cervical spine.



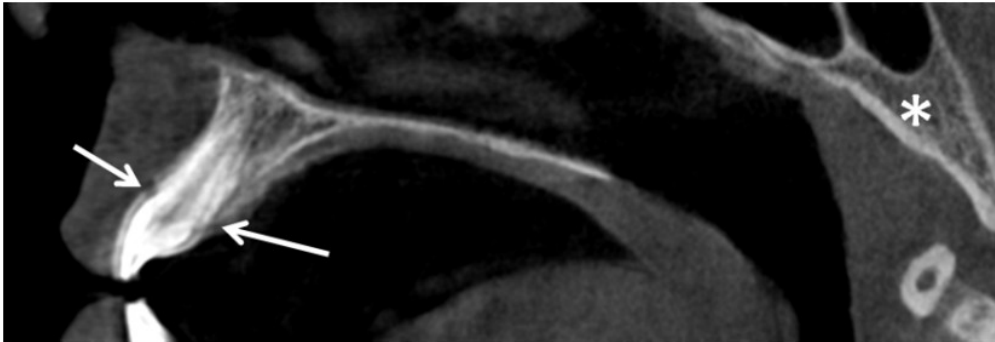
242  
243  
244  
245  
246  
247  
248  
249  
250  
251  
252  
253

**Fig. 12.** Patient 7. Head rotation from right to left, and translation from right to left. A. Axial view of the mandible. Arrow: thin streak tangent to the chin area of the mandible, and oriented to the left. B. 3D reconstruction of the mandible, view from the left side. Black arrows: 3D reconstruction of the double contour corresponding to streaks from A over the native mandible. Dotted arrows: double contour at the level of basilar cortical bone on the left side (corresponding to the translation from right to left).



254  
255  
256  
257  
258  
259  
260  
261  
262

**Fig. 13.** Patient 7. Head rotation from right to left, and translation from right to left. Axial view of the maxilla. Thin arrows: streaks tangent to vestibular side of the anterior teeth, and oriented to the left. Thick arrows: large stripes corresponding to the translation from right to left. Very thin arrow: U-shaped streak around vestibular face of lateral tooth crown, and oriented to the left. Dashed arrow: Y-shaped movement artifact of endodontic filling oriented to the left.



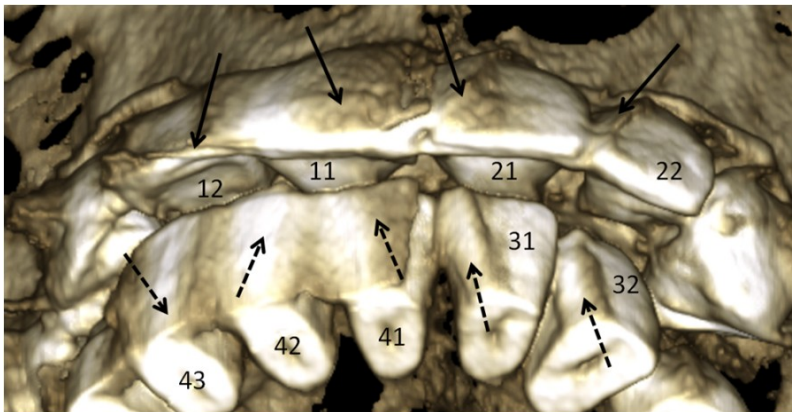
263  
264  
265  
266  
267  
268  
269  
270  
271  
272

**Fig. 14.** Patient 8. Head rotation from right to left, and translation from right to left. Sagittal view of the maxilla, and of the skull base. Arrows: double contour around maxillary front teeth. \* No movement at the level of the skull base.



273  
274  
275  
276  
277  
278  
279  
280

**Fig. 15.** Patient 8. Axial view of the maxilla. Head rotation from right to left, and translation from right to left. Arrows: streaks tangent to vestibular face of anterior teeth crowns. Streaks are oriented to the left. Dashed arrow: Y-shaped artifact of endodontic canal filling in tooth n°14 oriented to the left. Dotted arrows: stripes corresponding to the translation from right to left. Impossible to recognize the pulp chamber for right, and for left lateral teeth.



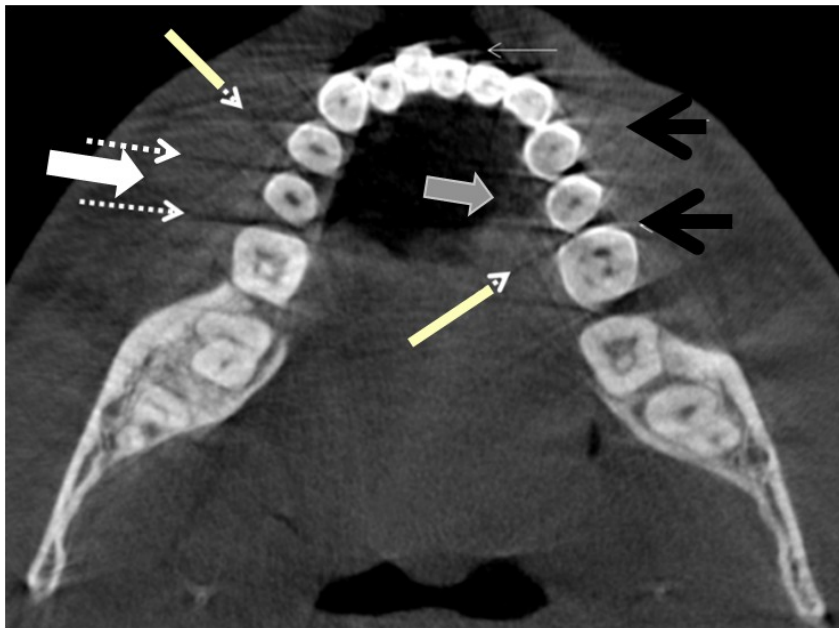
281  
282  
283  
284  
285  
286  
287

**Fig. 16.** Patient 8. 3D reconstruction of maxillary and mandibular anterior teeth. Black arrows: 3D reconstruction of streaks on vestibular side of teeth n°12, 11, 21, and 22. Streaks are oriented to the left. Dashed black arrows: 3D reconstruction of streaks on vestibular side of teeth n°43, 42, 41, 31, and 32. Streaks are oriented to the left.



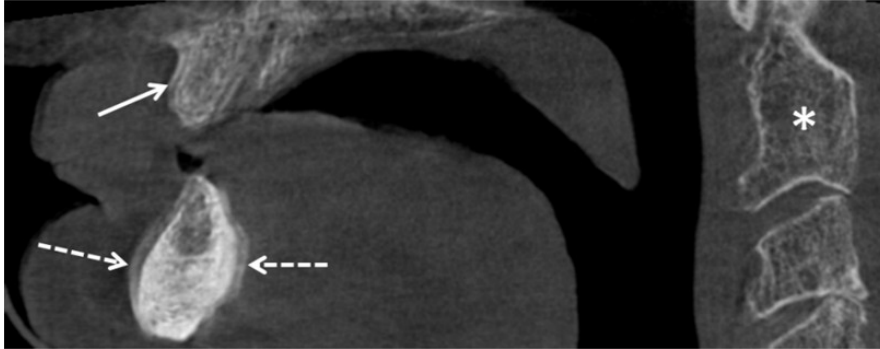
288  
289  
290  
291  
292

**Fig. 17.** Patient 9. Rotation of the head from right to left, and multiple direction translations from right to left. Sagittal view. Arrow: double contour around the chin area. \* No motion at the level of cervical spine.



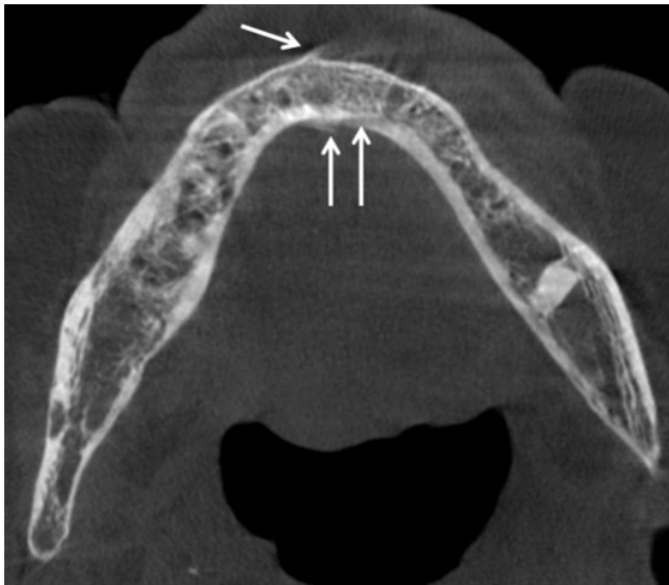
293  
294  
295  
296  
297  
298  
299  
300  
301  
302

**Fig. 18.** Patient 9. Rotation of the head from right to left, and multiple direction translations from right to left. Axial view of the mandible. Thin arrow: thin streak tangent to the vestibular side of the front teeth. Black arrows: streaks tangent to the lateral walls of teeth crowns. White big arrow: large stripe corresponding to the main translation from right to left. Dotted arrows: black streaks corresponding to the borders of large lateral stripes. Grey big arrow: large stripe corresponding to the main translation from right to left on lingual side. Thick white cream arrows: black streaks corresponding to other direction of translation.



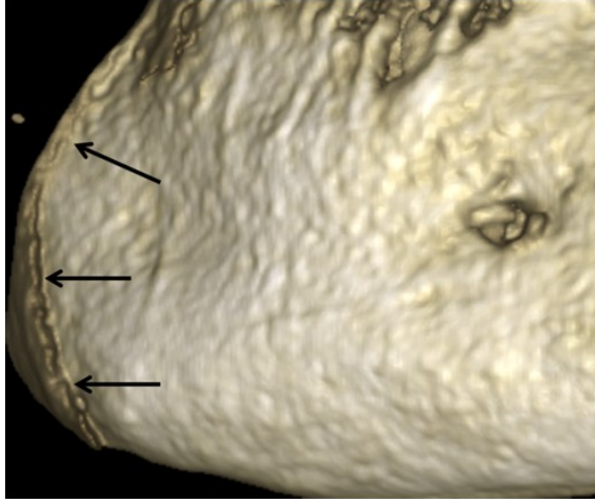
303  
304  
305  
306  
307  
308  
309

**Fig. 19.** Patient 10. Head rotation from right to left, and translation from right to left. Sagittal view of the maxilla, of the mandible and of the cervical spine. Complete edentulous patient. Dotted arrows: double contour on the Vestibular, and on lingual side in the midsagittal chin area. Arrow: minimal double contour at the level of the maxilla. \* No motion on cervical spine.



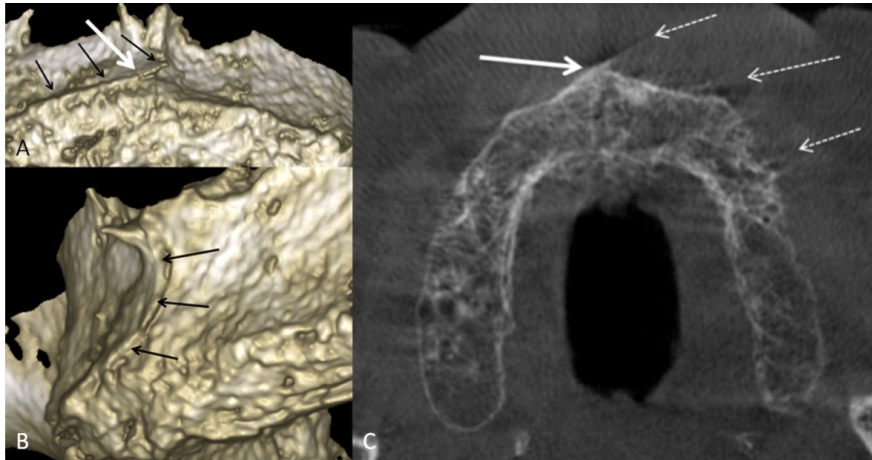
310  
311  
312  
313

**Fig. 20.** Patient 10. Axial view of the mandible. Head rotation from right to left, and translation from right to left. Arrow on vestibular side: streak tangent to the chin area. Two arrows on lingual side: duplication of lingual cortices.



314  
315  
316  
317  
318  
319

**Fig. 21.** Patient 10. Head rotation from right to left, and translation from right to left. 3D reconstruction of the chin area. Black arrows: line of streaks oriented from the right to the left superimposed on the vestibular mandibular chin.



320  
321  
322  
323  
324  
325  
326  
327  
328

**Fig. 22.** Patient 10. Head rotation from right to left at the level of the maxilla, and translation from right to left. A. 3D reconstruction of the anterior view of the maxilla. White arrow: streak tangent to the bone. Black arrows: 3D reconstruction of the streak tangent to the vestibular cortex. B. 3D reconstruction of the maxilla, a view from the left side. Black arrows: vertical part of the streak. C. Axial view of the maxilla. Arrow: streak tangent to the bone, at the same level as in A. Dashed arrows: multiple streaks arising from bone and oriented to the left side.



329  
330  
331  
332

**Fig. 23.** Patient 10. Head rotation from right to left, and translation from right to left. White arrows: double contour of the basilar cortical bone on the left side (translation from right to left).

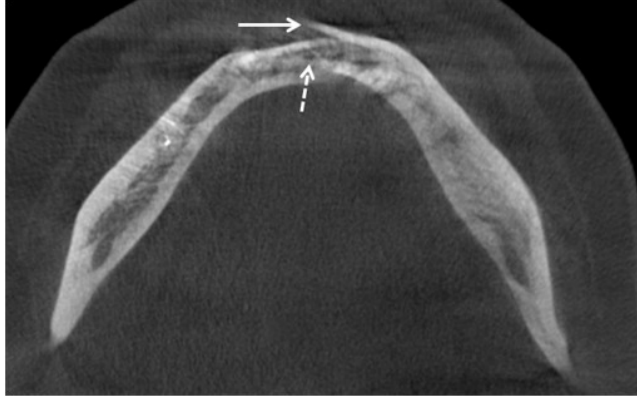
333

#### Motion artifacts of major level



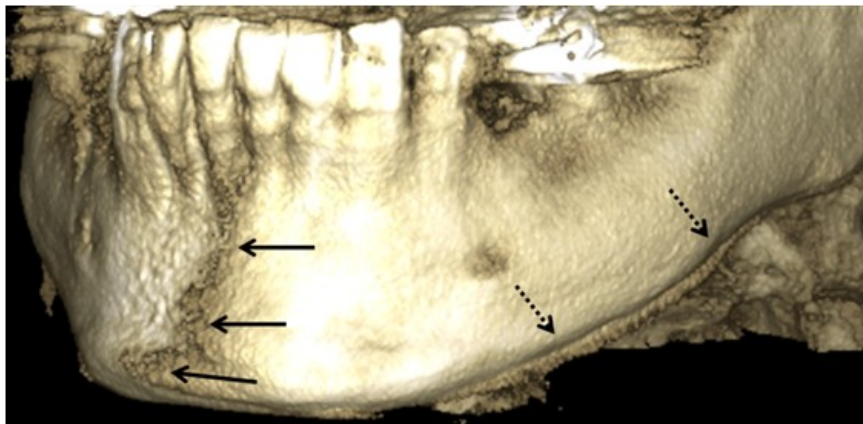
334  
335  
336  
337  
338  
339  
340  
341

**Fig. 24.** Patient 11. Sagittal view of the maxilla and of the mandible. Translation anterior-posterior of the head. Arrows: double contour of front teeth of the maxilla and mandible. Dotted arrow: anterior-posterior translation of the maxilla. Big arrow: anterior-posterior translation at the level of the mandibular chin. Big dashed arrow: double contour at the level of the floor of the mouth and of the tongue. Small dashed arrow: double contour of the hyoid bone. \* No motion at the level of cervical spine.



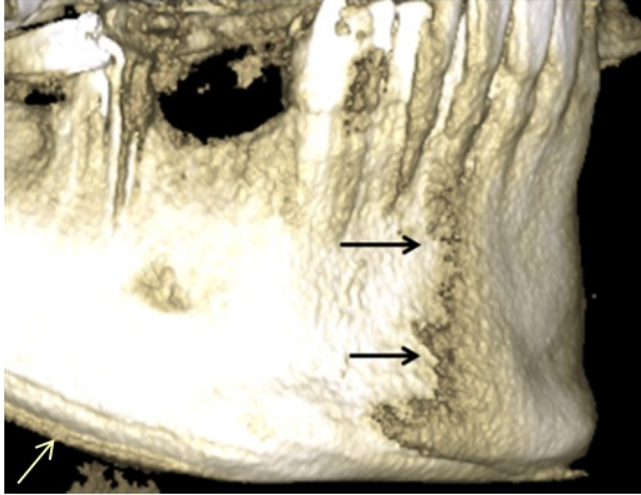
342  
343  
344  
345  
346  
347

**Fig. 25.** Patient 11. Anterior-posterior translation of the mandible. Arrow: major shift of vestibular cortical bone oriented to the right. Dashed arrow: major shift of lingual cortical bone oriented to the right. Shift of the left hemi-mandible over the right hemi-mandible.



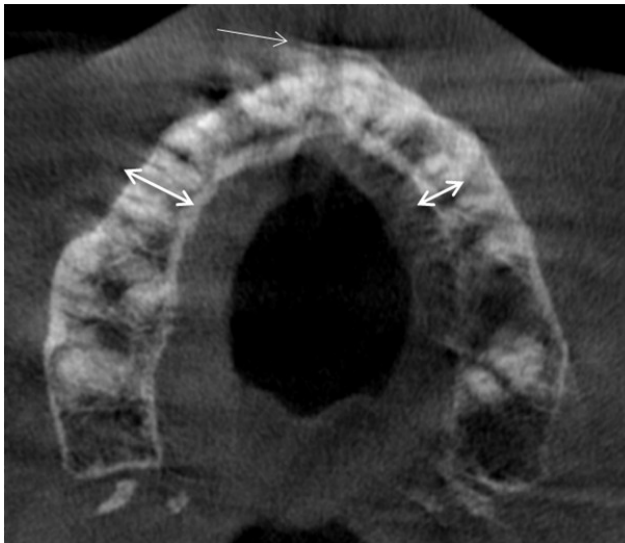
348  
349  
350  
351  
352  
353  
354

**Fig. 26.** Patient 11. Anterior-posterior translation of the mandible. 3D reconstruction of the mandible, left side. Black arrows: 3D reconstruction of left side vestibular cortex over the right side vestibular cortex. Black dotted arrows: duplication of the contour of the left mandibular basilar cortical bone (translation of the left mandible).



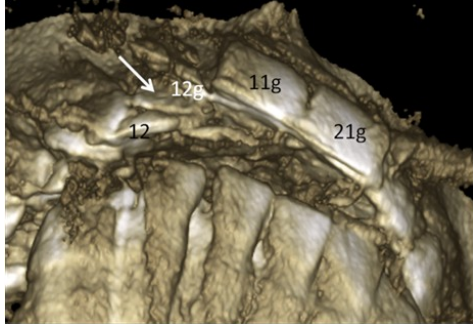
355  
356  
357  
358  
359  
360  
361

**Fig. 27.** Patient 11. Anterior-posterior translation of the mandible. 3D reconstruction of the mandible, right side. Black arrows: 3D reconstruction of left side vestibular cortical bone over the right side vestibular cortical bone. White arrow: duplication of the contour of the right mandibular basilar cortical bone (translation of the right mandible).



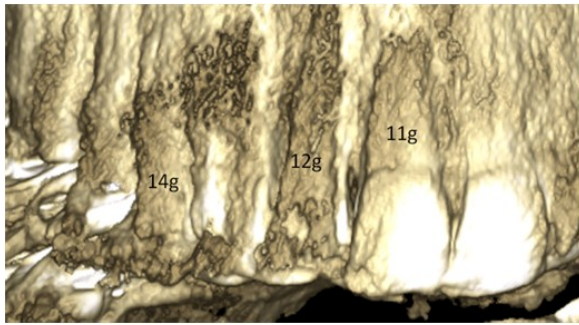
362  
363  
364  
365  
366

**Fig. 28.** Patient 11. Anterior-posterior translation of the maxilla. Arrow: shift of the left vestibular cortical bone over the right vestibular cortical bone. Elongation of teeth crowns on the right side. Shortening of teeth crowns on the left side. Global vanishing of dental structures on both dental arches.



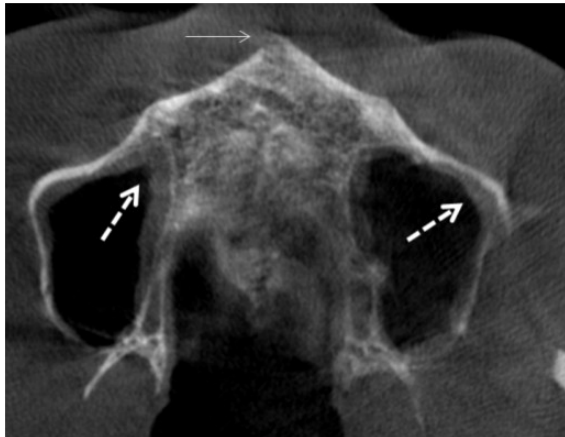
367  
368  
369  
370

**Fig. 29.** Patient 11. 3D reconstruction of the maxillary teeth. Ghost dental crowns (g) superimposed over true dental structures.



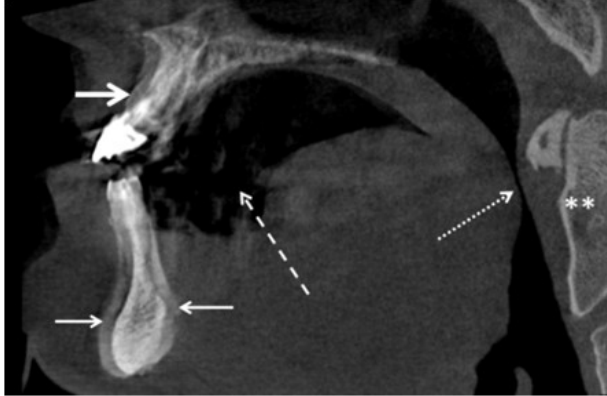
371  
372  
373  
374

**Fig. 30.** Patient 11. 3D reconstruction of the maxillary teeth. Ghost dental crowns and roots (g) superimposed over true dental structures.



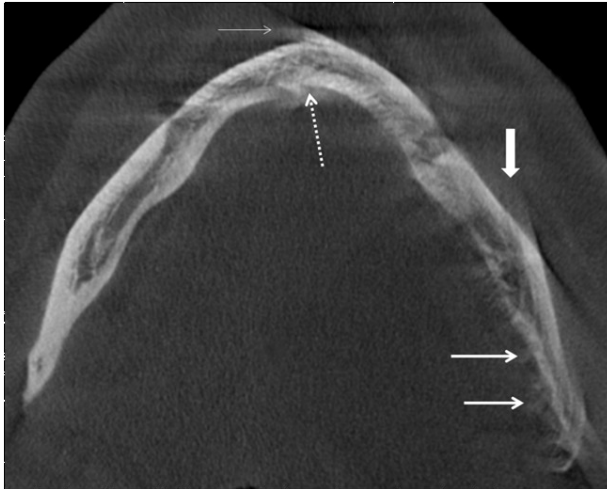
375  
376  
377  
378  
379

**Fig. 31.** Patient 11. Axial view of the maxilla at the level of maxillary sinus. Arrow: no shift of cortices at the level of anterior nasal spine. Dashed arrows: thickening of right and left maxillary sinus mucosa without duplication of contours, and still with possibility of correct radiological diagnosis.



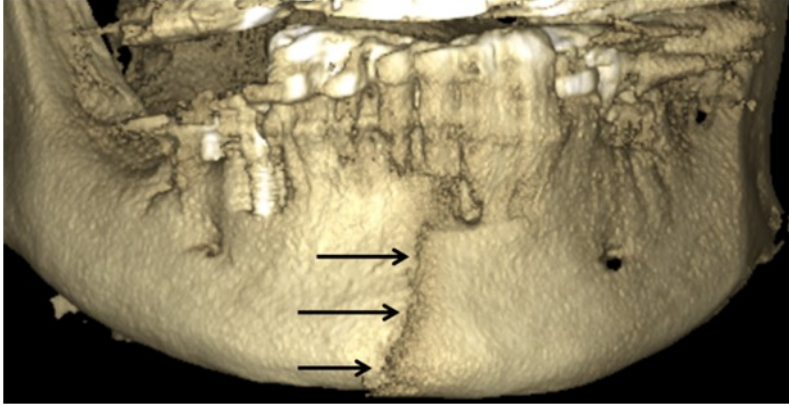
380  
381  
382  
383  
384  
385  
386  
387  
388

**Fig. 32.** Patient 12. Sagittal view of the maxilla, mandible, and cervical spine. Head anterior-posterior translation (multiple directions), and rotation of the head from left to right. Big arrow: double contour around the maxilla front teeth. Arrows: important double contour around the mandibular teeth, and around the chin area. Dashed arrow: recording of multiple motion directions at the tongue level. Dotted arrow: swallowing with soft palate blocking the nasopharynx. \*\* No motion at the level of the cervical spine.



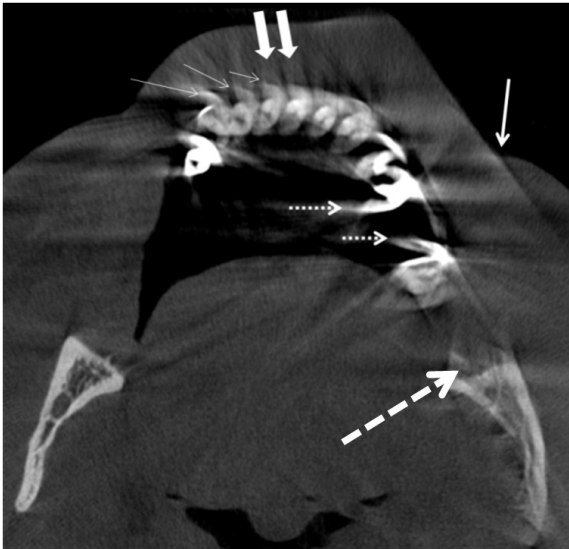
389  
390  
391  
392  
393  
394  
395  
396  
397

**Fig. 33.** Patient 12. Head anterior-posterior translation (multiple directions), and rotation of the head from left to right. Axial view of the mandible. Thin arrow: shift between hemi-mandible left and right on the midline, and the anterior shift of vestibular cortical bone on the midline. Dotted arrow: shift between hemi-mandible left and right on the midline, and the anterior shift of lingual cortical bone. Big arrow: stripe corresponding to a direction of vertical ramus translation. Arrows on left lingual side of the mandible: multiple "flame" streaks perpendicular to the lingual cortical bone.



398  
399  
400  
401  
402  
403

**Fig. 34.** Patient 12. Head anterior-posterior translation (multiple directions), and rotation of the head from left to right. 3D reconstruction of the mandible. Black arrows: anterior shift of left vestibular cortical bone oriented to the right.



404  
405  
406  
407  
408  
409  
410  
411  
412

**Fig. 35.** Patient 12. Head anterior-posterior translation (multiple directions), and rotation of the head from left to right. Thin arrows: ghost images of anterior teeth oriented to the right. Dotted arrows: U-shape metallic artifacts oriented to the right. Big dashed arrow: increased vestibular-lingual dimension of the left mandible. Loss of detail for bone marrow. Arrow: shift in soft tissues. Big arrows: stripes corresponding to another direction of anterior-posterior translation.

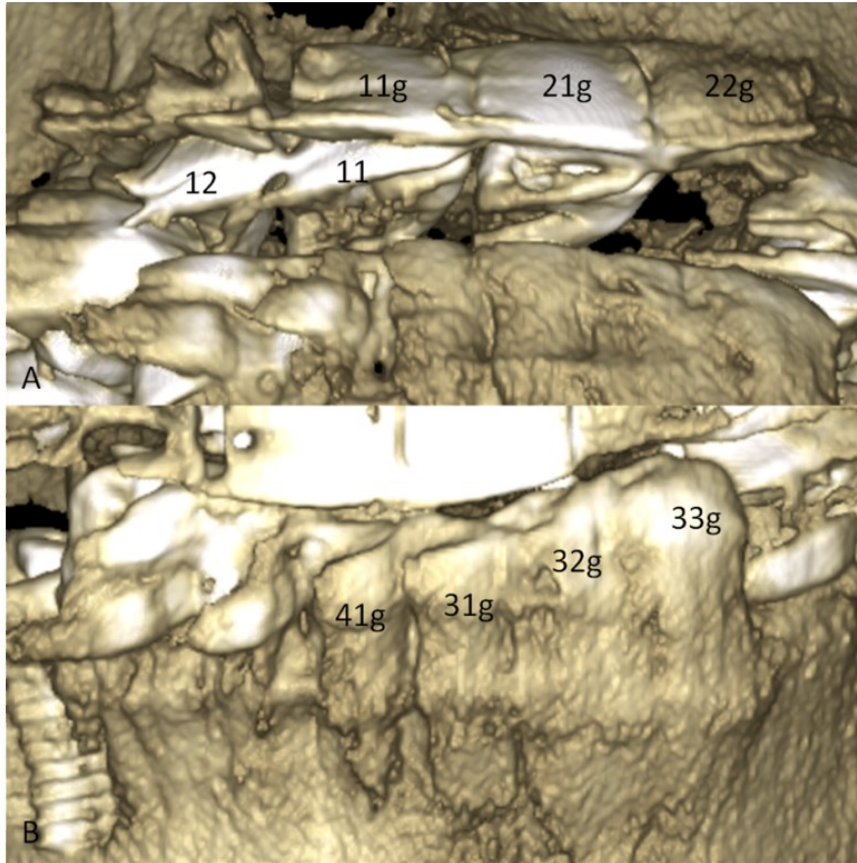
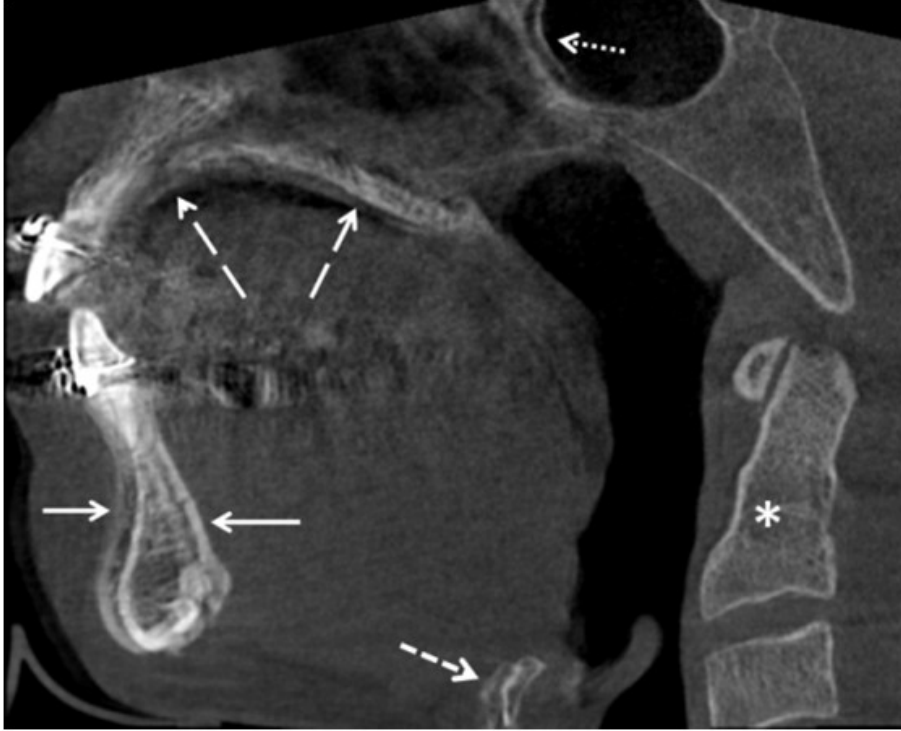


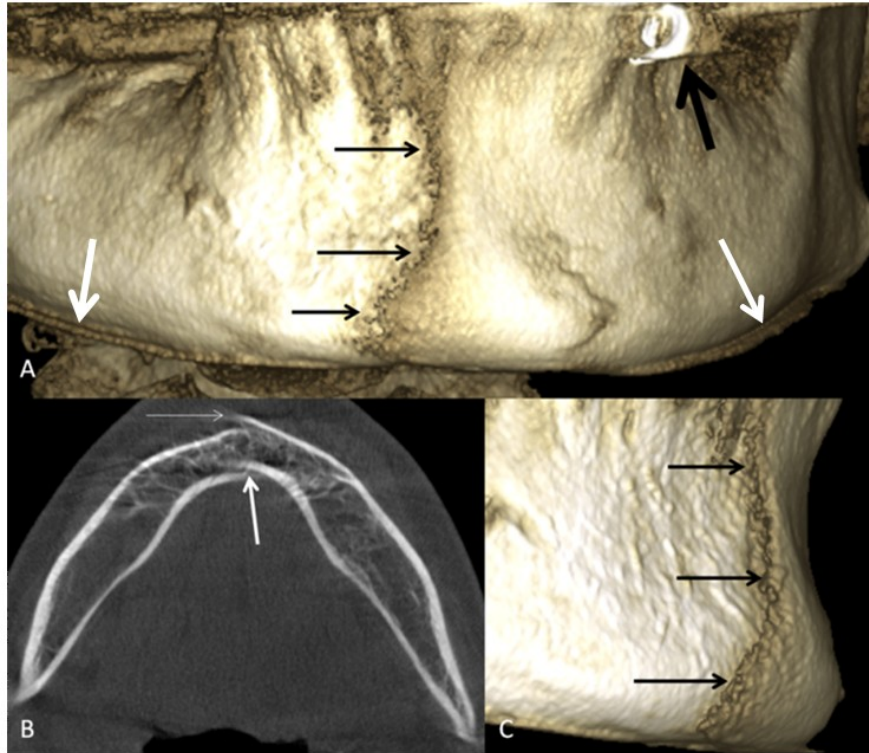
**Fig. 36.** Patient 12. Head anterior-posterior translation (multiple directions), and rotation of the head from left to right. A. 3D reconstruction of anterior teeth of the maxilla. Ghost representation of teeth (g) superimposed over true dental structures. B. 3D reconstruction of anterior teeth of the mandible. Ghost representation of teeth (g) superimposed over true dental structures.

413  
414  
415  
416  
417  
418  
419  
420  
421  
422  
423  
424  
425  
426  
427  
428



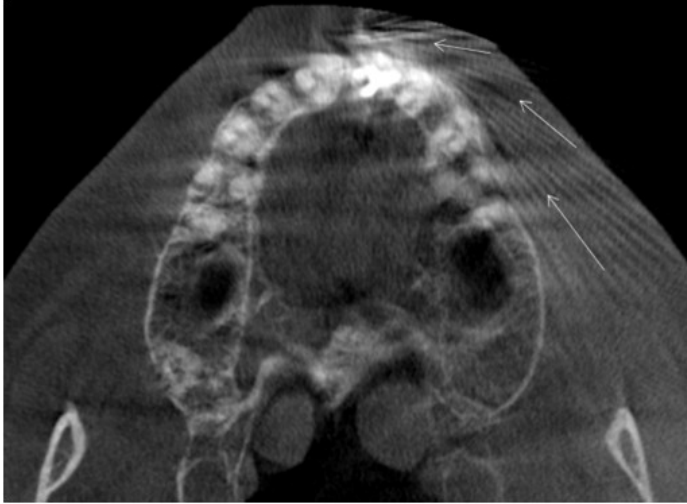
429  
430  
431  
432  
433  
434  
435  
436  
437  
438  
439  
440  
441  
442  
443  
444  
445  
446  
447  
448  
449  
450

**Fig. 37.** Patient 13. Head anterior-posterior translation. Sagittal view of mandible, maxilla, and of the cervical spine. Teeth with orthodontic braces. Arrows: double contour around the mandible. Small dashed arrow: double contour around the hyoid bone. Longer dashed arrows: double contour around the maxillary palate. \* No movement at the level of the cervical spine.



451  
 452 **Fig. 38.** Patient 13. Head anterior-posterior translation. A. 3D reconstruction  
 453 of the mandible. Black arrows: anterior shift of left vestibular cortical bone  
 454 oriented to the right. White arrows: double contour at the lingual basilar  
 455 cortical bone (corresponding to anterior-posterior translation). Black arrow:  
 456 metallic element belonging to orthodontic device. B. Axial view of the  
 457 mandible. Thin arrow: shift between left and right hemi-mandible on the  
 458 midline, and the anterior shift of vestibular cortical bone on the midline.  
 459 Arrow: shift between left and right hemi-mandible on the midline, and the  
 460 anterior shift of lingual cortical bone. C. 3D reconstruction of the mandible,  
 461 right view. Black arrows: anterior shift of left vestibular cortical bone super-  
 462 imposed over the right vestibular cortical bone, and oriented to the right.

463  
 464  
 465  
 466  
 467  
 468  
 469  
 470



471  
472  
473  
474  
475  
476

**Fig. 39.** Patient 13. Head anterior-posterior translation. Axial view of the maxilla. Thin arrows: “Comet tail” artifact in soft tissues on the left side, and associated with metallic element belonging to orthodontic device on the left mandible.



477  
478  
479  
480  
481  
482

**Fig. 40.** Patient 13. Head anterior-posterior translation. Axial view of the mandible. Thin arrows: “fireworks” artifact around the metallic element present in soft tissue on the right and left side. Arrows: metallic “fan” artifact oriented to the right side.

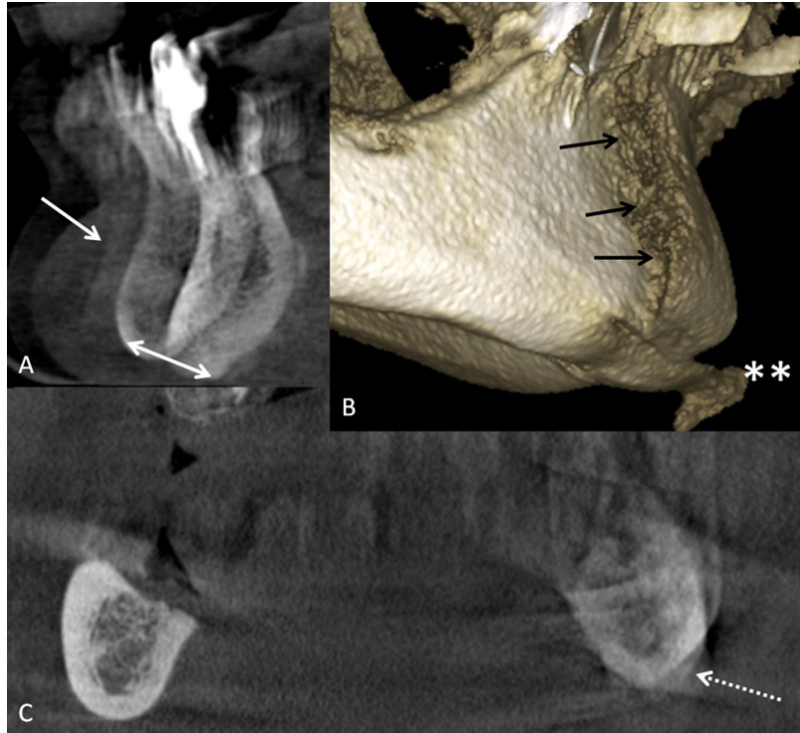


**Fig. 41.** Patient 14. Complex head rotation, and lateral translation from right to left. A. Important double contour of the mandible (double arrow). Arrow: triple contour of the mandible in the soft tissue. B. 3D reconstruction of the mandible. Black arrows: important anterior shift of left vestibular cortical bone superimposed over the right vestibular cortical bone, and oriented to the right. \*\* 3D reconstruction of complex rotation movement at the level of mandibular chin corresponding to the third contour from A. C. Coronal view of the mandible. Duplication of contour on the left mandible corresponding to the translation from right to left.

483  
 484  
 485  
 486  
 487  
 488  
 489  
 490  
 491  
 492  
 493  
 494  
 495  
 496  
 497  
 498  
 499  
 500  
 501  
 502  
 503  
 504

505



506

507

508

509

510

511

512

513

514

515

516

517

518

519

520

521

**Fig. 42.** Patient 14. Complex head rotation, and lateral translation from right to left. Thin arrow: major streak oriented to the right. Dotted arrows: "flame" artifacts on the lingual side of the left mandible. Big arrow: modification of the shape of the left compared to right mandible. Small arrows: multiple deformations of the surrounding soft tissues imaging. \*\* Movement at the level of the cervical spine.

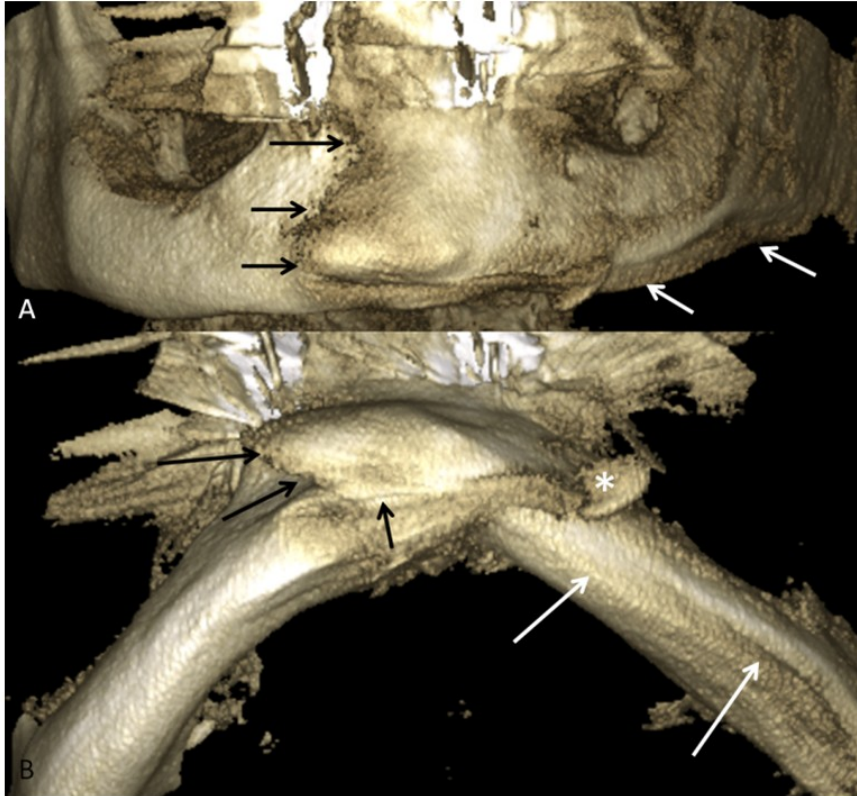
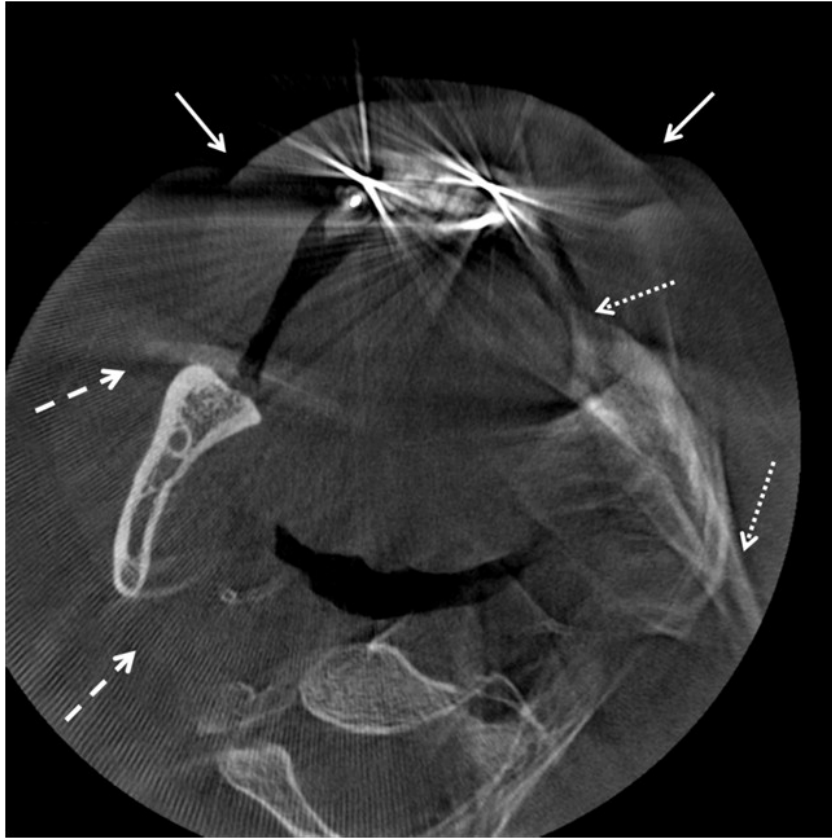


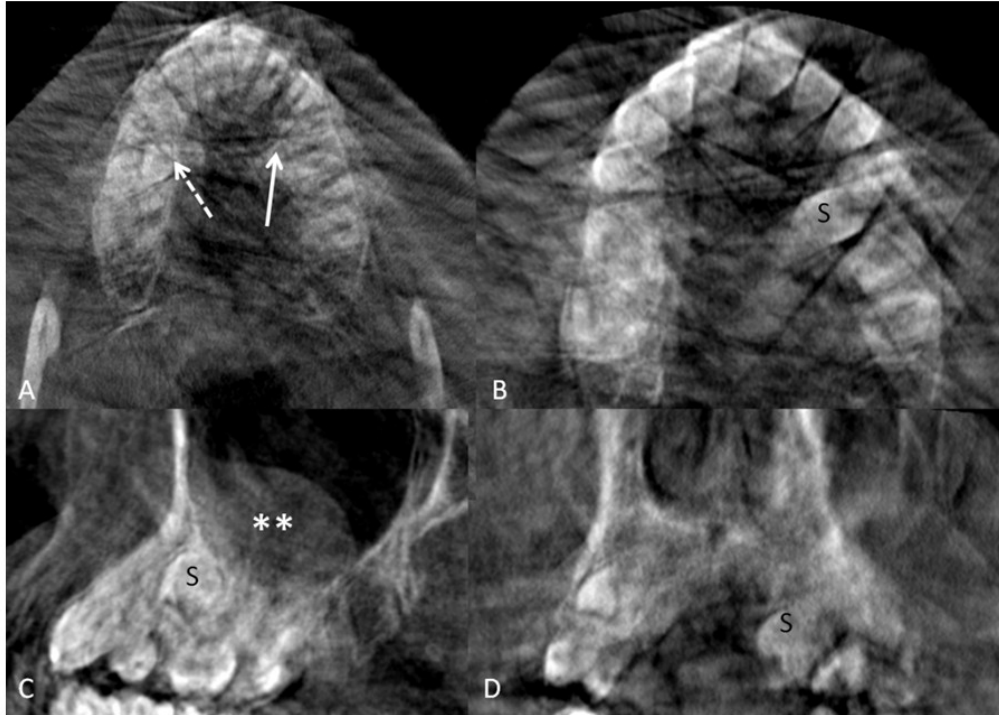
**Fig. 43.** Patient 14. Complex head rotation, and lateral translation from right to left. A. 3D reconstruction of the mandible, anterior view. Black arrows: important anterior shift of left vestibular cortex over the right vestibular cortical bone, and oriented to the right. White arrows: double contour of the lingual cortex on the left side corresponding to the translation from right to left. B. 3D reconstruction of the mandible, inferior view. Telescoping of right and left hemi-mandibles. Black arrows: important anterior shift of left vestibular cortical bone superimposed over the right vestibular cortical bone, and oriented to the right. \* 3D reconstruction of the third double contour on the left side. White arrows: double contour of the mandibular basilar cortical bone on the left side corresponding to the translation from right to left.

522  
 523  
 524  
 525  
 526  
 527  
 528  
 529  
 530  
 531  
 532  
 533  
 534  
 535  
 536  
 537  
 538  
 539  
 540  
 541



542  
543  
544  
545  
546  
547  
548  
549  
550  
551  
552  
553  
554  
555  
556  
557  
558  
559  
560

**Fig. 44.** Patient 14. Complex head rotation, and lateral translation from right to left. Axial view of the mandible. Dotted arrows: multiple centers of rotation inside the left mandible. Arrows: deformation of soft tissues surrounding the mandible. Dashed arrows: aliasing artifact. Presence of "stars" metallic artifacts on anterior teeth due to addition of metal and movement artifacts.



561  
562  
563  
564  
565  
566  
567  
568  
569  
570

**Fig. 45.** Patient 15. Complex head multiple rotation and translation movements during scanning. “Hatched” image artifact. A. Axial view of the maxilla. Dashed arrow: supernumerary tooth n°15’ on the right side of the palate. Arrow: suspected supernumerary tooth n°25’ on left side of the palate. B. Axial view of the maxilla. S: supernumerary tooth n°25’ on left side of palate. C. Sagittal view of the maxilla. S: supernumerary tooth n°25’ on left side of the palate. \*\* Mucous retention pseudocyst in the left maxillary sinus. D. Frontal view of the maxilla. S: supernumerary tooth n°25’ on left side of the palate.

571

## Discussion

572  
573  
574  
575  
576  
577  
578  
579  
580

There is a scarce open access/open knowledge resources on motion artifacts in dentomaxillofacial CBCT in medical literature [article 24], and therefore our null hypothesis was accepted. Instead of general description of stripe-like, ring-like patterns, double bone contours, and lack of sharpness of images [1] we found a much greater range of different types of motion artifacts (Table 1).

581

**Table 1.** Types of motion artifacts related to the level of image degradation.

Low level	Intermediary level	Major level
Duplication of contour in the midsagittal area	Loss of pulp chamber image for premolars and molars	Double contour at the level of the floor of the mouth, the tongue, the hyoid bone, cervical spine
Streaks tangent to the vestibular cortical bone	Large stripe in soft tissue lateral to lateral teeth (lateral translation)	Major anterior shift of hemi-vestibular cortical bone over the over side
Streaks tangent to the vestibular side of anterior teeth	3D reconstructed streaks on the vestibular side of teeth	Duplication of the contour of the right and left mandibular basilar cortical bone
3D reconstruction of the motion streaks tangent to the vestibular cortex, "pseudo-fracture"	Double contour at the level of basilar cortical bone (lateral translation)	Global vanishing of dental structures on both dental arches
Y-shaped artifact of the endodontic root filling	U-shaped streak around vestibular face of lateral tooth crown	Ghost images of dental crowns over true dental structures
	Black streaks corresponding to other direction of translation (limited "hatched" image)	"Flame" streaks perpendicular to the lingual cortex (multiple translations)
		"Comet tail" metal and motion artifact
		"Fireworks" metal and motion artifact
		"Stars" metal and motion artifacts
		Deformations of the surrounding soft tissues imaging
		"Hatched" image artifact (complex rotation and translation motion)

582

583

584

585

586

587

588

589

590

591

592

Few in vitro studies [4, 16, 17] provide with explanation of motion artifacts produced in CBCT. Rolling motion artifact seems to have the most disturbing effect on the diagnostic quality of the image [16]. However, that study used Newtom CBCT where the patient is in lying position [16]. The majority of CBCT devices use a sitting or standing position where translation motion is also possible to occur. We used Planmeca Promax3D Mid device. Two elements are provided to block the head in this type of CBCT. There exists a head positioning and locking plate with screw around the parietal bones of the skull, and a chin plastic support for the mandible. In this system the head cannot translate vertically in coronal plane (up-down), cannot rotate anteriorly or posteriorly (nodding) in the sagittal plane, and cannot rotate

593 laterally (from right to left and vice versa) in the coronal plane (tilting).  
594 However, the upper head positioning plate with blocking screw could be not put on  
595 maximum on the patient head because of the pain expressed by the patient, because  
596 of a great amount of natural hair or because of ethnical hairdressing. In those  
597 situations the head presents with much more freedom for motion during CBCT  
598 examination. Therefore, the anterior-posterior translation in sagittal plane, the  
599 translation right-left in axial plane, and the rotation in axial plane (rolling) are  
600 possible.

601 The second source of motion artifact during CBCT scanning is related to the circular  
602 pathway of the detector and of the generator around the patient. In Planmeca Promax  
603 3D mid, the detector is much closer to the patient than the generator, and it moves  
604 from left to right. During the scanning time the detector is first close to the patient  
605 right shoulder, then to the upper back and to the back of the head, and at the end it is  
606 close to the right shoulder. If the detector touch the shoulders or the back of the head  
607 during the acquisition time the patient may move the body and the head to avoid the  
608 detector obstacle, and it will induce the rotation motion artifact. This problem can  
609 occur with patients with short neck, with kyphosis, and especially if the mandible  
610 volume is needed to be scanned. Posterior-anterior head motion artifact could be  
611 induced when the detector touches the back of the head. It may happen with some  
612 kind of hairdressings, dreadlocks, clips in hair under veil, and wigs. Moreover, some  
613 patients with major mandibular prognathism may present with important anterior-  
614 posterior head length. In those patients the back of the head may enter in contact  
615 with the moving detector. Multiple rotations and translations may occur for patients  
616 with specific conditions such as diverse types of dementia, Parkinson disease, head  
617 tremor, claustrophobia or mental disability. Patients in severe pain presenting  
618 advanced osteonecrosis (post radiotherapy, on biphosphonates) in the mandible, or  
619 with facial fractures may not be able to stand without motion during scanning time.  
620 Patients on wheelchairs, in sitting position, may also present global instability, and  
621 present with complex motion artifacts.

622 In our illustrated review we found that low level motion artifacts were more related  
623 to head rotation in axial plane (rolling). Rolling and lateral translation were  
624 responsible of intermediary level motion artifacts. Major level motion artifacts were  
625 created by complex motion with multiple rotation axes, multiple translation  
626 directions, and anteroposterior translation. Each level above low level presented  
627 with the accumulation of previous artifacts, and shown new types of artifacts related  
628 to each level.

629 The possibility of clinical diagnosis with images artefacted by motion depends of the  
630 anatomical area of interest. Even a small rotation motion degrades the quality of  
631 tooth image, of tooth surroundings, and of anatomy of dental canals (Figures 1, 8)  
632 which corresponds also with findings from the study of Moratin et al. [4]. However,  
633 the images with major level motion artifacts may still serve for sinus diagnosis (Fig-  
634 ure 31) and for supranumerary teeth anatomical location description (Figure 45).

635 The prevention seems the best choice as correction algorithms are of very limited  
636 help for intermediary and major level motion artifacts. Each patient should receive

637 clear explanation about motion artifacts, and do not move during the entire scanning  
 638 time. Head locking plates should be closed as much as possible around the head.  
 639 Patients with hairdressings, wigs, and dreadlocks should have their hair put around  
 640 the neck and as much on the front. If possible hair clips should be taken off under  
 641 veils. Patient with obvious kyphosis, major prognathism, craniofacial syndrome,  
 642 should be discarded from standing or sitting CBCT, and CT scan should be proposed  
 643 instead. A presentation of the CBCT device and a test rotation without patient  
 644 should be shown to patients with claustrophobia to gain their trust in the device, and  
 645 in the surroundings. Standing stability of patients with dementia, Parkinson disease,  
 646 head tremor or mental disability should be evaluated case by case. Some patients can  
 647 sit in the device instead of stand. In Planmeca Promax 3D Mid we can also use a  
 648 ultra low dose protocol with a time of scanning of 6 seconds. This protocol is used  
 649 for children but it can also be used to avoid motion artifacts in disabled patients.  
 650 Patients with severe pain or with facial fracture may be discarded and be send to CT  
 651 scan as emergency situation.  
 652 The main limitation of this study is related to empirical observation of patient  
 653 motion and to correlation of this observation with obtained artifacted images.  
 654 However, more robust methodology should be developed possibly exploring  
 655 virtual 3D simulation of various directions of movements (rotation, translation, and  
 656 complex motion) and of length of time of movement on virtual skull images during  
 657 CBCT scanning time to validate the patient observation findings from this initial  
 658 study [16, 17].

659

- 660 • **Acknowledgements:** none  
 661 • **Funding sources statement:** this study does not received any funding  
 662 • **Competing interests:** Prof R. Olszewski is Editor-in-Chief of Nemesis  
 663 • **Ethical approval:** We obtained the approval from our Ethical committee for  
 664 this study (B403/2019/03DEC/542)  
 665 • **Informed consent:** There was no need for informed consent for this study

666 **Authors contribution:**

Author	Contributor role
Olszewski Raphael	Conceptualization, Data curation, Investigation, Methodology, Resources, Validation, Writing original draft preparation, Supervision, Writing review and editing

667

668

## References

669

1. Spin-Neto R, Wenzel A. Patient movement and motion artefacts in cone beam computed tomography of the dentomaxillofacial region: a systematic literature review. *Oral Surg Oral Med Oral Pathol Oral Radiol* 2016;121:425-433.

670

671

672

673

674

675

676

677

678

679

680

681

682

683

684

685

686

687

688

689

690

691

692

693

694

695

696

697

698

699

700

701

702

703

704

705

706

707

708

10. Hebda A, Theys S, de Roissart J, Perez E, Olszewski R. Contribution of dental private practitioners to publications on anatomical variations using cone beam

- 709 computed tomography. *Nemesis* 2020;14:1-54.  
710
- 711 11. Olszewski R. Artifacts related to cone beam computed tomography (CBCT)  
712 technology and their significance for clinicians: illustrated review of medical  
713 literature. *Nemesis* 2020;11:1-29.  
714
- 715 12. Spin-Neto R, Costa C, Salgado DM, Zambrana NR, Gotfredsen E, Wenzel A.  
716 Patient movement characteristics and the impact on CBCT image quality and  
717 interpretability. *Dentomaxillofac Radiol* 2018;47:20170216.  
718
- 719 13. Yıldız Keriş E. Effect of patient anxiety on image motion artefacts in CBCT.  
720 *BMC Oral Health* 2017;17:73.  
721
- 722 14. Spin-Neto R, Matzen LH, Schropp L, Gotfredsen E, Wenzel A. Movement  
723 characteristics in young patients and the impact on CBCT image quality.  
724 *Dentomaxillofac Radiol* 2016;45:20150426.  
725
- 726 15. Nagarajappa AK, Dwivedi N, Tiwari R. Artifacts: The downturn of CBCT  
727 image. *J Int Soc Prev Community Dent* 2015;5:440-445.  
728
- 729 16. Nardi C, Molteni R, Lorini C, Taliani GG, Matteuzzi B, Mazzoni E, Colagrande  
730 S. Motion artefacts in cone beam CT: an in vitro study about the effects on the  
731 images. *Br J Radiol* 2016;89:20150687.  
732
- 733 17-Spin-Neto R, Mudrak J, Matzen LH, Christensen J, Gotfredsen E, Wenzel A.  
734 Cone beam CT image artefacts related to head motion simulated by a robot skull:  
735 visual characteristics and impact on image quality. *Dentomaxillofac Radiol*  
736 2013;42:32310645.  
737  
738
- 739  
740